Chem. Soc. Rev., 1987, **16**, 467—498

Angular Geometries and other Properties of Hydrogen-bonded Dimers: A Simple Electrostatic Interpretation of the Success of the Electron-pair Model

By A. C. Legon
DEPARTMENT OF CHEMISTRY, UNIVERSITY OF EXETER, STOCKER ROAD, EXETER, EX4 4QD
D. J. Millen
CHRISTOPHER INGOLD LABORATORIES, DEPARTMENT OF CHEMISTRY, UNIVERSITY COLLEGE LONDON, 20 GORDON STREET, LONDON WC1H 0AJ

1 Introduction

The aim of this article is to set out a simple theoretical justification for a set of rules, based on *n*-bonding and π-bonding electron pairs, for predicting angular geometries of isolated (*i.e.* unperturbed by lattice or solvent interactions) hydrogen-bonded dimers. The rules have proved very successful in accounting for a very wide range of angular geometries. We show below, first, that the angular geometry of the hydrogen-bonded dimer is determined largely by the angular variation of the electrostatic potential in the vicinity of the acceptor atom in the molecule B. Secondly, we show that the angular variation of the electrostatic potential correlates well with the angular disposition of nonbonding electron pairs in the sense employed in the VSEPR model of Gillespie and Nyholm.[1] Thus, essentially we are relating the experimental angular geometries of hydrogen-bonded dimers to the simple nonbonding (or π-bonding) pair model of the acceptor molecule B that now has a familiar place in all modern textbooks of Chemistry. We must emphasize that we are *not* attempting to prove that nonbonding pairs exist as 'rabbit's ears' or 'water wings'. Indeed, we shall make it clear that conventional diagrams representing nonbonding pairs in this way are, at very least, gross exaggerations. Nevertheless, we find in all cases examined that the potential energy of a nonperturbing electrophilic probe in the vicinity is a minimum along just those directions normally associated with the axes of nonbonding (or π-bonding) pairs, as conventionally envisaged by chemists (see ref. 1, for example). Given that the calculated electrostatic potential in the vicinity of B is accurate, it follows from this result that the nonbonding pair model of B contains the essence of the full electrostatic description.

This correlation between the angular geometries predicted by the nonbonding pair model of B and the electrostatic description of B is further improved if the angular variation of the potential energy of HF, when viewed as an extended electric dipole, is considered instead of the electrostatic potential. Not only do these findings together provide a theoretical foundation for the experimentally successful rules but they allow a corollary to the rules to be formulated, *i.e.* that the direction

[1] R. J. Gillespie and R. S. Nyholm, *Quart. Rev., Chem. Soc.*, 1957, **11**, 339.

of the HF molecule in a weakly bound dimer B · · · HF acts as a probe for the direction of *n*- or π-bonding pairs on B. We shall also show that the electrostatic approach provides a valuable basis for rationalizing several other properties of hydrogen-bonded dimers.

In achieving the above aim, we first (Section 2) present a brief account of selected angular geometries of isolated hydrogen-bonded dimers together with a summary of the techniques used to determine them. Secondly, we enunciate in Section 3 the rules for predicting angular geometries and compare the predictions with key results from Section 2. The third stage of this article provides, through consideration of the electric charge distributions of molecules B and HX, evidence for the presence of, and angular disposition of, nonbonding (and π-bonding) pairs on B (Section 4). We then proceed in Section 5 to discuss electrostatic models for the dimers B · · · HF. We begin with the simplest case in which the HF molecule is modelled by a point positive charge alone (*i.e.* the F end of the molecule is ignored). We next treat HF as an extended electric dipole $H^{\delta+}$–$F^{\delta-}$ before going on to discuss the more complete model, due to Buckingham and Fowler, in which the electric charge distribution of HF is described fully. In Section 5, we also briefly discuss the quantum mechanical justification of the electrostatic model before considering in Section 6 some further applications of the model to account for the lengthening of HF bonds on formation of B · · · HF and the ease of angular and radial distortion of the geometry from the equilibrium position. Finally, we demonstrate on the basis of experimental evidence that even for the most strongly bound dimers (*e.g.* H_3N · · · HCl) it is correct to write the valence bond description of the dimer essentially as B · · · HX, with relatively little contribution from the ionic structure $\overset{+}{B}H\ \overset{-}{X}$.

2 Experimental Angular Geometries of Hydrogen-bonded Dimers B · · · HX

A. Introduction.—We define the angular geometry of a hydrogen-bonded dimer B · · · HX to be the relative orientation of two essentially rigid molecular subunits B and HX. It turns out that the angular geometry of B · · · HX molecules is distorted with little cost in energy and therefore it is crucial to determine such geometries for isolated dimers B · · · HX unperturbed by lattice or solvent interactions. This means working at low pressure in the gas phase. To date rotational spectroscopy has been the most useful method of determining such geometries for isolated dimers. We first summarize the various techniques used, then present a tabulation of selected angular geometries of B · · · HF as determined by these techniques.

B. Techniques used to Determine the Angular Geometries of Isolated Dimers B · · · HX.—The angular geometries of dimers B · · · HX discussed in this review have all been determined by rotational spectroscopy and therefore refer to the isolated species. Rotational spectra have been observed either in low pressure gas mixtures of B and HX at equilibrium or in supersonically expanded jets or beams composed of B and HX diluted in *e.g.* argon. In all, three techniques have been used: Stark-modulation microwave spectroscopy, molecular-beam electric-resonance

spectroscopy (MBERS), and pulsed-nozzle, Fourier-transform microwave spectroscopy.

(i) *Stark-Modulation Microwave Spectroscopy.* Low-resolution rotational spectra of a number of dimers B • • • HF have been recorded in equilibrium gas mixtures by using a Hewlett-Packard 8460A 33 kHz Stark-modulated microwave spectrometer employing phase-sensitive detection.[2] The control of the temperature of the microwave absorption cell was a crucial operation in these experiments because, on the one hand, as low a temperature as possible was required to favour the dimer but, on the other hand, condensation of the mixture placed a lower limit on the working temperature. Temperatures in the range -70 to -30 °C were commonly used and were achieved by cooling with liquid nitrogen. The gold-plated absorption cell was enclosed by an insulated jacket into which liquid nitrogen could be pumped, at a rate controlled by a sensing platinum resistance thermometer, from a Cryoson pressurized dewar. The liquid nitrogen was delivered at eight points onto a baffle plate above the absorption cell *via* a branching system of polythene pipes insulated with foam rubber. Since most of this work involved dimers B • • • HF, the gold plating of the inner surface of the absorption cell was a significant advantage.

(ii) *Molecular-beam Electric Resonance Spectroscopy.* The MBERS technique has been reviewed a number of times.[3,4] Basically, inhomogeneous electric fields are used to deflect molecules, through the Stark effect, from beams of the supersonically expanded mixture of B and HX in argon. This effect depends strongly on the rotational state of the dimer and hence electric dipole transitions are detected by altering the trajectories of the dimers that have suffered a rotational transition. As a consequence, only molecules that have certain trajectories are allowed to reach the detector which is usually a mass spectrometer. The number of dimers reaching the detector as a function of the radiation frequency yields the required spectrum.

(iii) *Pulsed-nozzle, Fourier-transform Microwave Spectroscopy.* This method involves the Fourier-transform microwave spectroscopy of a pulse of gas mixture (B and HX diluted in, say, argon) expanded supersonically from a nozzle into an evacuated Fabry-Pérot cavity.[5] The microwave pulse induces a macroscopic polarization in the gas when it is in collisionless expansion between the Fabry-Pérot mirrors. It is required that the half-life, T_2, for the decay of the macroscopic polarization is much greater than that (τ_c) for the decay of the microwave pulse within the Fabry-Pérot cavity. Accordingly, when the polarized dimers in the cold gas ($T \approx 5$ K) begin to emit at some rotational transition frequency and the detector is opened, the microwave pulse has dissipated and only the molecular emission survives to be detected. Details of the theory and operation of this technique have been described.[6]

[2] A. C. Legon, D. J. Millen, and S. C. Rogers, *Proc. R. Soc. London, Ser. A*, 1980, **370**, 213.
[3] T. R. Dyke, *Top. Curr. Chem.*, 1984, **120**, 85.
[4] T. R. Dyke and J. S. Muenter, in 'International Review of Science, Physical Chemistry Series Two', ed. A. D. Buckingham, Butterworths, London, 1975; Vol. 2.
[5] T. J. Balle and W. H. Flygare, *Rev. Sci. Instrum.*, 1981, **52**, 33.
[6] See for example, A. C. Legon, *Annu. Rev. Phys. Chem.*, 1983, **34**, 275.

(iv) *Advantages and Disadvantages of the Three Techniques.* The three techniques used to detect and measure the rotational spectra of hydrogen-bonded dimers have their own advantages and disadvantages but are in several respects complementary. Although Stark modulation microwave spectroscopy has been restricted mainly to moderately strongly hydrogen-bonded dimers and has moderate resolution, it has the significant advantage that rotational spectra are obtained in vibrationally excited states of the low-lying hydrogen-bond modes as well as in the vibrational ground state. Vibrational satellites are important because of the information they contain about the hydrogen-bond potential energy function and this can be crucial in deciding upon the equilibrium angular geometry, as for example in $H_2O \cdots HF$.[7] The pulsed-nozzle, Fourier-transform and MBERS methods have, on the other hand, a very high sensitivity for molecular dimers and a high resolution because of the low effective temperature of the gas pulse and because the emission/absorption of radiation occurs while the gas is in collisionless expansion. Very weakly bound molecular dimers can be investigated with these instruments. A concomitant disadvantage of the low effective temperature is, however, that spectra in the vibrational ground state only are observed. The equilibrium and MBERS methods, through the Stark effect, readily furnish electric dipole moments of dimers, while the high resolution of the pulsed-nozzle, Fourier-transform and MBERS methods allow the investigation of nuclear quadrupole and nuclear spin–nuclear spin coupling effects. Such information is often complementary to the more usual principal moments of inertia as a tool for determining the angular geometry of B · · · HX.

C. Classification of Experimental Angular Geometries of B · · · HX

In this section, we shall classify the angular geometries of isolated hydrogen-bonded dimers by referring to the experimental results (determined as above) for some carefully selected, key dimers. We shall restrict our attention to dimers of the type B · · · HF for two reasons, but nevertheless we believe that the discussion that follows is generally applicable to dimers B · · · HX where X = Cl, Br, or CN. First, HF is the proton donor in by far the largest class of dimers investigated and, secondly, the HF molecule has some electrical properties that will be particularly advantageous when, later, we discuss how hydrogen-bonded dimers of the type B · · · HX provide a basis for locating nonbonding electron pairs on molecules B.

The classification of the angular geometries of dimers B · · · HF is conveniently made with the aid of Table 1 in which we give the experimental geometries, and appropriate references for the key dimers.[2,7–20] The table is divided into two sections: that (*a*) containing dimers in which the HF molecule forms a hydrogen bond to a nonbonding electron pair on B and that (*b*) containing dimers in which the HF molecule forms a hydrogen bond to a π-bond or pseudo-π bond on B.

Section (*a*) is subdivided into classes that are defined according to the geometrical arrangement at the acceptor atom in B. The first of these consists of dimers having a linear heavy atom arrangement. Many linear dimers B · · · HX are

[7] Z. Kisiel, A. C. Legon, and D. J. Millen, *Proc. R. Soc. London, Ser. A*, 1982, **381**, 419.

Table 1 *Experimental angular geometries of some selected hydrogen-bonded dimers* B · · · HF

B	*Experimental angular geometry*		*References*
(a) n-bonding type			
HCN	linear	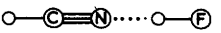	2,8
H_2CO	trigonal at O	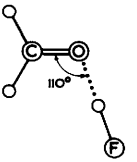	9
H_2O^a	pyramidal at O	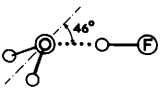	7,10
	pyramidal at O	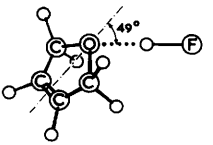	11
	pyramidal at O	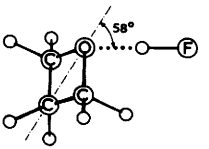	12
	pyramidal at O	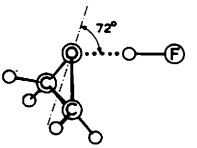	13
H_2S	pyramidal at S	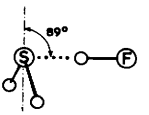	14,15
SO_2	trigonal, with *cis* arrangement with respect to central S=O bond	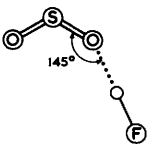	16,17

(b) π-bonding type

H–C≡C–H	T-shaped	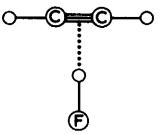	18
$H_2C{=}CH_2$	HF lies along the bisector of the C=C bond, perpendicular to molecular plane	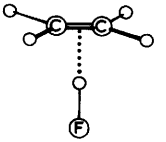	19
▽	HF lies along a median of the cylopropane triangle	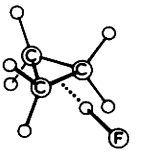	20
			20

[a] The angle φ, which is the angle between the C_2 axis of B and the O ··· H–F line, is 46(8)° for B = H_2O and the correspondingly defined angles are given for B = 2,5-dihydrofuran. oxetane, oxirane, and H_2S

known, but we use only the example HCN ··· HF,[2,8] Other examples include OC ··· HCl,[21] MeCN ··· HF,[22,23] HCN ··· HCN,[24,25] and PH_3 ··· HF.[26] The second class consists of dimers B ··· HF in which there is a trigonal arrangement of bonds around the acceptor atom in B, as exemplified by H_2CO ··· HF.[9] The third

[8] A. C. Legon, D. J. Millen, and L. C. Willoughby, *Proc. R. Soc. London. Ser. A*, 1985, **401**, 327.
[9] F. A. Baiocchi and W. Klemperer, *J. Chem. Phys.*, 1983, **78**, 3509.
[10] J. W. Bevan, Z. Kisiel, A. C. Legon, D. J. Millen, and S. C. Rogers, *Proc. R. Soc. London. Ser. A*, 1980, **372**, 441.
[11] R. A. Collins, A. C. Legon, and D. J. Millen, *J. Mol. Struct.*, 1987, **162**, 31.
[12] A. S. Georgiou, A. C. Legon, and D. J. Millen, *J. Mol. Struct.*, 1980, **69**, 69.
[13] A. S. Georgiou, A. C. Legon, and D. J. Millen, *Proc. R. Soc. London. Ser. A*, 1981, **372**, 511.
[14] R. Viswanathan and T. R. Dyke, *J. Chem. Phys.*, 1982, **77**, 1166.
[15] L. C. Willoughby, A. J. Fillery-Travis, and A. C. Legon, *J. Chem. Phys.*, 1984, **81**, 20.
[16] A. J. Fillery-Travis and A. C. Legon, *Chem. Phys. Lett.*, 1986, **123**, 4.
[17] A. J. Fillery-Travis and A. C. Legon, *J. Chem. Phys.*, 1986, **85**, 3180.
[18] W. G. Read and W. H. Flygare, *J. Chem. Phys.*, 1982, **76**, 2238.
[19] J. A. Shea and W. H. Flygare, *J. Chem. Phys.*, 1982, **76**, 4857.
[20] L. W. Buxton, P. D. Aldrich, J. A. Shea, A. C. Legon, and W. H. Flygare, *J. Chem. Phys.*, 1981, **75**, 2681.
[21] P. D. Soper, A. C. Legon, and W. H. Flygare, *J. Chem. Phys.*, 1981, **74**, 2138.
[22] J. W. Bevan, A. C. Legon, D. J. Millen, and S. C. Rogers, *Proc. R. Soc. London. Ser. A*, 1980, **370**, 239.
[23] P. Cope, A. C. Legon, D. J. Millen, and L. C. Willoughby, *J. Chem. Soc., Faraday Trans. 2*, 1986, **82**, 1197.
[24] K. Georgiou, A. C. Legon, D. J. Millen, and P. J. Mjöberg, *Proc. R. Soc. London, Ser. A*, 1985, **399**, 377.
[25] E. J. Campbell. L. W. Buxton, and W. H. Flygare, *Chem. Phys.*, 1981, **56**, 399.
[26] A. C. Legon and L. C. Willoughby, *Chem. Phys.*, 1983, **74**, 127.

class is particularly important in the discussion presented in the remainder of this article and is composed of dimers B···HF in which the corresponding arrangement is pyramidal. The final class consists of dimers like SO_2···HF,[16,17] in which the possibility of two distinguishable arrangements about the acceptor atom exists.

3 Rules for Predicting Angular Geometries of B···HX and Comparison of the Predictions with Experiment

A. Introduction.—We presented a set of rules in 1982[27] which were generalizations of our experimental observations on a carefully selected but limited subset of key hydrogen-bonded dimers. The rules have subsequently proved to be extremely valuable for predicting angular geometries of a wide range of classes (*e.g. n*- and π-type) of dimers B···HX and are therefore well established. We now present the rules and then compare, for a representative range of B···HX, the predicted and observed angular geometries.

B. The Rules.—The rules rely on the identification of nonbonding and π-bonding electron pairs on the acceptor molecule B, and these are taken to determine the direction of the hydrogen bond. The hydrogen atom in HX is electrophilic and is assumed to seek the most electron-rich region in B. The most common electron-rich, or nucleophilic, regions will be along the axes of nonbonding or π-bonding electron pairs. Hence, the gas-phase equilibrium geometry of a dimer B···HX can be obtained by assuming that:

(*i*) *the axis of the HX molecule coincides with the supposed axis of a nonbonding electron pair as conventionally envisaged,*

or, if B has no nonbonding electron pairs but has π-bonding electron pairs,

(*ii*) *the axis of the HX molecule intersects the internuclear axis of the atoms forming the π-bond and is perpendicular to the plane of symmetry of the π-bond.*

Rule (*i*) is definitive when B has both nonbonding and π-bonding pairs.

C. Comparison of Predictions from Rule (*i*) with Experiment.—In this section, we compare with experiment the predictions of angular geometries of B···HX made on the basis of rule (*i*), *i.e.* when the acceptor atom in B carries nonbonding electron pairs. Furthermore, we subdivide our discussion according to the number of equivalent or inequivalent nonbonding pairs.

(i) *One nonbonding pair on the acceptor atom of B.* Many examples in this class are known. We select as representative the dimers HCN···HF,[2,8] OC···HCN,[28] and H_3N···HCl[29,30] and illustrate schematically in Figure 1 the single nonbonding electron pair and the direction of the hydrogen bond in each case. Our diagrams of nonbonding pairs throughout are of the conventional, schematic type

[27] A. C. Legon and D. J. Millen, *Discuss. Faraday Soc.*, 1982, **73**, 61.
[28] E. J. Goodwin and A. C. Legon, *Chem. Phys.*, 1984, **87**, 81.
[29] E. J. Goodwin, N. W. Howard, and A. C. Legon, *Chem. Phys. Lett.*, 1986, **131**, 319.
[30] N. W. Howard and A. C. Legon, *J. Chem. Phys.*, to be published.

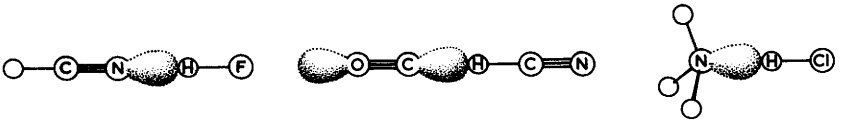

Figure 1 *Schematic diagrams illustrating the axially symmetric angular geometries predicted for hydrogen-bonded dimers formed by molecules B that carry a single nonbonding electron pair on the acceptor atom in B*

illustrating the angular distribution function. We note that of the two nonbonding pairs in CO, that carried by C is apparently the more nucleophilic because all dimers formed by CO and HX so far investigated have the order OC • • • HX of the nuclei.

(ii) *Two Equivalent Nonbonding Electron Pairs on the Acceptor Atom of B.* The prototype molecule in this class is of course $H_2O \cdots HF$.[7,10] The experimental investigations have shown unambiguously that the equilibrium structure is pyramidal at oxygen but with only a very small potential energy barrier ($\approx$ 1.5 kJ mol^{-1}) to inversion through the planar configuration, as is clear from the experimentally determined potential energy function shown in Figure 2. We note that because of the proximity of the zero-point level to the top of the barrier, the molecule can be described as *effectively* planar in the zero-point state. Nevertheless, the *equilibrium* geometry is unambiguously pyramidal, with the angle φ = 46(8)°

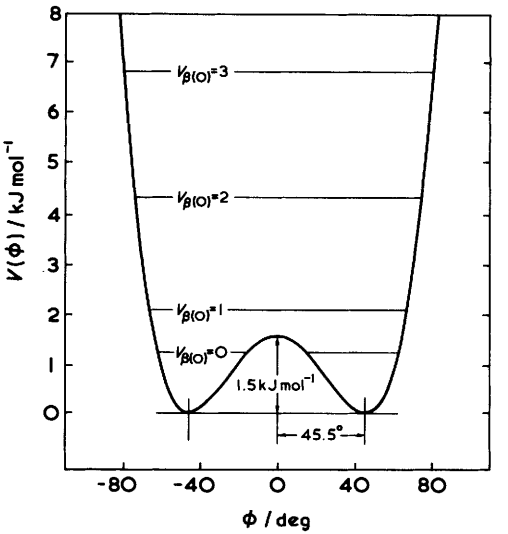

Figure 2 *Effective one-dimensional potential energy function for the low frequency, out-of-plane bending mode* $\nu_{\beta(O)}$ *in* $H_2O \cdots HF$. φ *is the angle between the* H–F *direction and the bisector of the* HOH *angle of* H_2O

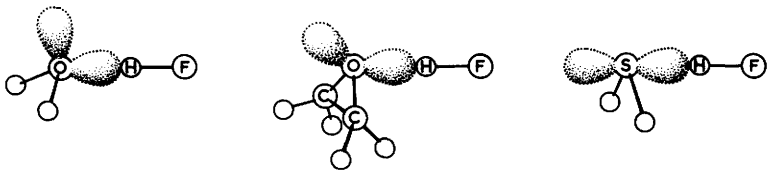

Figure 3 *Schematic diagrams illustrating the pyramidal angular geometries predicted for hydrogen-bonded dimers formed by molecules B that carry two equivalent nonbonding electron pairs on the acceptor atom in B*

between the bisector of the HOH angle and the HF bond direction. Such an arrangement is clearly consistent with the rules, as shown with the aid of a schematic diagram of the *n*-pairs on O in H_2O in Figure 3. A similar arrangement has been observed for $(H_2O)_2$.[31] The reason for the two equivalent minima in Figure 2 is immediately apparent from the model shown in Figure 3. On the other hand, discussion of why the potential energy barrier to the planar form is so low must be postponed until Section 4C(ii).

A question of immediate chemical interest is: what happens as the angle between the two equivalent nonbonding pairs on oxygen is increased? This can be tested in a systematic manner by considering the series of dimers B • • • HF where B = H_2O, 2,5-dihydrofuran, oxetane, or oxirane, the experimentally determined angular geometries of which are displayed in Table 1. We note that the angle φ (see Table 1 for definition) increases from 46(8)° where B = H_2O, through 49° for B = 2,5-dihydrofuran, 58° for B = oxetane, to 72° when B = oxirane. This is just the order expected from the VESPR model[1] of ROR compounds since the angle ROR decreases along the series and therefore the angle between the *n*-pairs is predicted to increase commensurately. The *n*-pair model for oxirane • • • HF is included in Figure 3. The experimental geometries for the series B • • • HF with B = H_2O, 2,5-dihydrofuran, oxetane, or oxirane were of great importance in establishing the rules. Similarly, the *n*-pair model of H_2S in which the nonbonding electrons occupy *sp* hybrid orbitals predicts an L-shaped angular geometry (see Figure 3) for H_2S • • • HF. When the angular geometry was subsequently determined,[14] the angle φ was found to be 89° (see Table 1), a result that inspired further confidence in the rules.

Another important type of dimer in which the acceptor atom carries two equivalent nonbonding pairs is exemplified by H_2CO • • • HX. The rules predict, on the basis of the usual electronic model of formaldehyde, a trigonal planar arrangement at the oxygen atom in H_2CO • • • HF, (see Figure 4). The experimental result[9] (see Table 1) confirms this prediction and indeed leads to an angle COF = 110° which is close to the model value of 120°.

(iii) *Two Inequivalent Nonbonding Electron Pairs on the Acceptor Atom of B.* As in formaldehyde, the rules predict a trigonal planar arrangement at the oxygen atom

[31] T. R. Dyke and J. S. Muenter, *J. Chem. Phys.*, 1974, **60**, 2929.

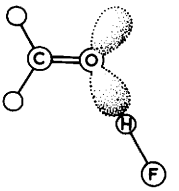

Figure 4 *Schematic diagram illustrating the trigonal planar angular geometries predicted for hydrogen-bonded dimers formed by molecules B that carry two equivalent nonbonding electron pairs on the acceptor atom in B*

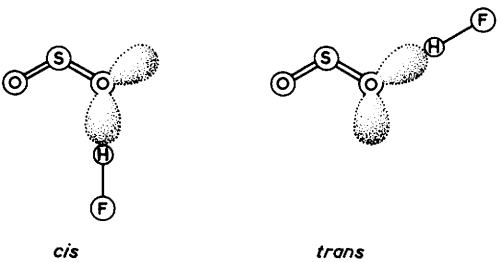

Figure 5 *Schematic diagrams illustrating the* cis *and* trans *trigonal planar isomers of* $SO_2 \cdots HF$ *predicted on the basis of the nonbonding pair rules. In this case the acceptor atom in* SO_2 *carries two inequivalent nonbonding electron pairs*

for a hydrogen-bonded dimer of the type $SO_2 \cdots HF$ formed between SO_2 and HF. Two isomers of such a dimer are possible, depending on whether the HF molecule lies along the axis of the *n*-pair that is *trans* to the other S=O bond or *cis* to it, as illustrated in Figure 5. The rules are noncommital in respect of these possibilities. The observed geometry[16,17] of $SO_2 \cdots HF$ is indeed trigonal, planar at oxygen (see Table 1) in accordance with the rules and, so far, only the *cis* isomer has been observed, indicating that the *cis* nonbonding pair is the more nucleophilic. (iv) *Three equivalent nonbonding electron pairs on the acceptor atom of B.* A detailed investigation of the HF dimer and its deuterated species[32,33] establishes a non-linear geometry in which the HF subunit acting as the proton acceptor makes an angle of *ca.* 70° with the F ··· F axis. The electron pair model predicts just such an angular geometry, as shown in Figure 6. The sum of the electron distribution functions for the three nonbonding pairs will of course yield an axially symmetric distribution.

D. Comparison of Predictions from Rule (*ii*) **with Experiment.**—When π-bonding pairs but no nonbonding pairs are present on the acceptor molecule B, as in

[32] T. R. Dyke, B. J. Howard, and W. Klemperer, *J. Chem. Phys.*, 1972. **56**. 2442.
[33] B. J. Howard, T. R. Dyke, and W. Klemperer, *J. Chem. Phys.*, 1984. **81**, 5417.

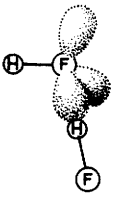

Figure 6 *Schematic diagram illustrating the angular geometry predicted for* HF · · · HF *on the basis of the nonbonding pair rules. In this case, the acceptor* F *atom carries three inequivalent nonbonding electron pairs*

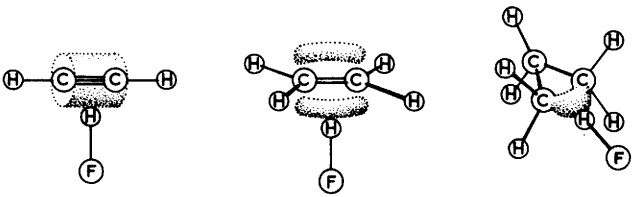

Figure 7 *Schematic diagrams illustrating the angular geometries predicted for dimers in which a hydrogen bond is formed to a* π *or pseudo-*π *bonding electron pair on the acceptor molecule B*

ethylene, rule (*ii*) predicts that in the equilibrium geometry of B · · · HX the axis of the HX molecule intersects the internuclear axis of the atoms forming the π-bond and is perpendicular to the plane of symmetry of the π-orbital. The familiar π-bond model for ethylene is shown in Figure 7 and the observed geometry[19] of ethylene · · · HF in Table 1. The latter is as predicted by the rules.

Acetylene can be considered to have two equivalent π-bonding electron pairs which then lead to a π electron density consistent with the known cylindrical symmetry, and can be represented conventionally as shown in Figure 7. The rules straightforwardly predict a T-shaped geometry, as implied in Figure 7 for acetylene · · · HF, which is as observed.[18] Acetylene is a member of the same isoelectronic series as HCN, N_2, and CO. In the dimers B · · · HF where B is HCN, N_2, or CO the acceptor molecule has in each case π-bonding as well as nonbonding electron pairs. In view of the linear geometry established for each dimer[2,8,34,35] the proton evidently prefers to seek the axis of the nonbonding pair rather than the region of high π-electron density. Acetylene, on the other hand, has no nonbonding pairs and hence can form only the weaker π-bonded dimer.

Cyclopropane, historically, has often been considered to behave in some ways like an unsaturated hydrocarbon. A model that exhibits pseudo-π electron density and bent C–C single bonds has been put forward by Coulson and Moffitt[36] to

[34] P. D. Soper, A. C. Legon, W. G. Read, and W. H. Flygare, *J. Chem. Phys.*, 1982, **76**, 292.
[35] A. C. Legon, P. D. Soper, and W. H. Flygare, *J. Chem. Phys.*, 1981, **74**, 4944.
[36] C. A. Coulson and W. E. Moffitt, *Philos. Mag.*, 1949, **40**, 1.

account for such behaviour. This model is included (for one C–C bond) in Figure 7. Application of the rules requires an HF molecule to lie at equilibrium along a median of the cyclopropane equilateral triangle in this model since then it samples the maximum pseudo-π electron density. The observed geometry[20] of cyclopropane • • • HF (Table 1) is indeed just as predicted by the rules.

E. Effect of Weakening the Hydrogen Bond on the Angular Geometry of *n*-Type Dimers.—The above discussion demonstrates that for dimers B • • • HF at least, the nonbonding electron pairs are dominant in determining the direction of the hydrogen bond and therefore in determining the angular geometry. But dimers B • • • HF are relatively strong and the B • • • H distance is relatively short. An interesting question concerns the evolution of the angular geometry as the hydrogen bond is weakened. This question can be answered by reference to dimers of the type B • • • HCN.

It has been established experimentally[37] that HCN, acting as a hydrogen-bond donor, forms weaker and longer bonds than HF. For the purposes of this discussion we shall consider the dimers B • • • HX, where B = oxirane or formaldehyde and X is F or CN. Experiment demonstrates that when X = F, the configurations at oxygen are permanently pyramidal (oxirane)[13] or trigonal (formaldehyde)[9] with no inversion doubling resolvable in the rotational spectra and leads to the angles given in Table 1. By contrast, the dimers B • • • HCN show evidence of inversion doubling for both B = oxirane[38] and B = formaldehyde,[39] with the corresponding angles 52.2° and 138°, respectively. The B • • • HCN are therefore of *effective* C_{2v} symmetry, *i.e.* an effectively planar zero-point geometry for the heavy atoms in oxirane • • • HCN and an effectively linear arrangement C=O • • • HCN in formaldehyde • • • HCN, but the equilibrium conformation is still pyramidal. Such results are as expected if, in the limit of a weak hydrogen bond, the short-range directional effect of the nonbonding electron pairs on O are diminished and the longer range dipole–dipole interaction becomes predominant. Nevertheless, the nonbonding pairs still have an effect and a simple dipole–dipole model is even in these cases inadequate for predicting the *equilibrium* geometry. Occasionally, as in SO_2 • • • NCH[40] and CO_2 • • • NCH,[41] the hydrogen bond interaction becomes so weak that other interactions between B and HX are stronger and the lowest energy conformer is 'antihydrogen' bonded.

4 Evidence Supporting the Nonbonding and π-Bonding Electron Pair Model of the Acceptor Molecule B

A. Introduction.—The rules introduced in Section 3 for predicting angular geometries of B • • • HX are essentially electrostatic in character. In the crudest approximation, the hydrogen atom of HX is viewed as the electrophile which seeks

[37] A. C. Legon and D. J. Millen, *J. Am. Chem. Soc.*, 1987, **109**, 356.
[38] E. J. Goodwin, A. C. Legon, and D. J. Millen, *J. Chem. Phys.*, 1986, **85**, 676.
[39] E. J. Goodwin and A. C. Legon, *J. Chem. Phys.*, 1987, **87**, 2426.
[40] E. J. Goodwin and A. C. Legon, *J. Chem. Phys.*, 1986, **85**, 6828.
[41] K. R. Leopold, G. T. Fraser, and W. Klemperer, *J. Chem. Phys.*, 1984, **80**, 1039.

the direction of maximum electron density in B. The most common regions of high nucleophilicity are along the axes of nonbonding or π-bonding electron pairs, as conventionally envisaged by chemists. In fact, electrostatic models of hydrogen-bonded dimers B • • • HX have extensive history.

As early as 1933, Bernal and Fowler[42] put forward a point-charge electrostatic model for the interaction between water molecules. Lennard-Jones and Pople,[43] recognizing the importance of the nonbonding electron pair contributions to the electric dipole moment of water, provided a basis for understanding the directional character of hydrogen bonds in terms of a point-charge model in which a proton donor is attracted to a negatively charged site provided by a nonbonding electron pair. Coulson[44] later published an influential paper describing a quantum mechanical theory of the hydrogen bond in which he recognized four terms contributing to the interaction energy: electrostatic, delocalization, dispersion, and repulsive terms. The question of the relative importance of each of the terms, or closely related terms arising in similar schemes for partitioning the total energy, has subsequently attracted much attention.[45–47] The importance of the electrostatic contribution has been frequently emphasized and so too has the directional character of nonbonding electron pairs.[48] On the other hand, some authors[49] have emphasized a molecular orbital view of the hydrogen bond and the merits of a HOMO–LUMO model.[50]

During the last decade, three developments have further advanced our understanding of the hydrogen bond. First, there has become available an extensive body of evidence about geometries (and other properties) of hydrogen-bonded dimers B • • • HX, largely through rotational spectroscopy.[3,51] Secondly, theoretical developments have made it possible to describe accurately the electrostatic charge distributions of monomers and therefore to calculate the electrostatic energy of interaction between B and HX.[47,52,53] Finally, *ab initio* calculations can now provide geometries of simple hydrogen-bonded dimers with useful accuracy and can also allow the interaction energy, including its angular dependence, to be partitioned reliably, so making it possible to test the angular dependence of the electrostatic energy.

We have already surveyed in Section 2C the first of these developments, namely the experimentally determined angular geometries of dimers B • • • HX. In this Section, we now proceed to examine the electrostatic basis of the empirical rules (Section 3C) for predicting angular geometries using nonbonding and π-bonding pair models of B.

[42] J. D. Bernal and R. H. Fowler, *J. Chem. Phys.*, 1933, **1**, 515.
[43] J. Lennard-Jones and J. A. Pople, *Proc. R. Soc. London. Ser. A*, 1951, **205**, 155.
[44] C. A. Coulson, *Research (London)*, 1957, **10**, 149.
[45] P. A. Kollman, *J. Am. Chem. Soc.*, 1977, **99**, 4875.
[46] P. Schuster, *Angew. Chem., Int. Ed. Engl.*, 1981, **20**, 546.
[47] H. Umeyama and K. Morokuma, *J. Am. Chem. Soc.*, 1977, **99**, 1316.
[48] J. E. Del Bene, *J. Chem. Phys.*, 1973, **58**, 3139.
[49] G. C. Pimental and A. L. McClellan, 'The Hydrogen Bond', W. H. Freeman, San Francisco, 1960.
[50] F. A. Baiocchi, W. Reiher, and W. Klemperer, *J. Chem. Phys.*, 1983, **79**, 6428.
[51] A. C. Legon and D. J. Millen, *Chem. Rev.*, 1986, **86**, 635.
[52] G. J. B. Hurst, P. W. Fowler, A. J. Stone, and A. D. Buckingham, *Int. J. Quantum Chem.*, 1986, **29**, 1223.
[53] A. P. L. Rendell, G. B. Bacskay, and N. S. Hush, *Chem. Phys. Lett.*, 1985, **117**, 400.

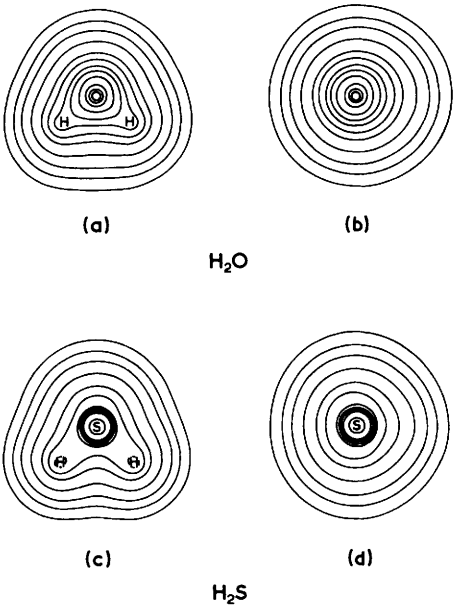

Figure 8 *Total electron density maps for:* (*a*) H_2O *in the molecular plane;* (*b*) H_2O *in the nonbonding-pair plane perpendicular to the molecular plane, and bisecting the* H–O–H *angle;* (*c*) H_2S *in the molecular plane; and* (*d*) H_2S *in the nonbonding-pair plane*
(Redrawn from ref. 54 with permission of the American Chemical Society)

B. Evidence from Electron-density Contour Maps.—We begin our account of the evidence by examining electron-density contour maps for the directions of nonbonding pairs. Reliable electron-density contour maps are available for small molecules from *ab initio* calculations. We show in Figure 8 such maps for H_2O and H_2S.[54] In each case, a section in the plane of the molecule and a section perpendicular to the molecular plane but containing the molecular symmetry axis is shown. When we examine in Figure 8 the section in the plane containing the nonbonding pair axes in H_2O, we find no evidence for increased electron density along the expected direction. At first sight this seems surprising when compared with Figure 3, but it must be noted that the nonbonding pairs illustrated schematically in Figure 3 are enormously exaggerated and that realistic diagrams would show only a tiny deviation from a hemispherical charge distribution on, for example, the oxygen atom of H_2O. This tiny deviation from a hemispherical distribution is indeed reflected in the very small difference (~ 1.5 kJ mol^{-1}) between the energies of the planar and equilibrium pyramidal forms of $H_2O \cdots HF$ (see Figure 2). Nevertheless, this deviation is clearly sufficient to define the equilibrium

[54] J. Bicerano, D. S. Marynick, and W. N. Lipscomb, *J. Am. Chem. Soc.*, 1978, **100**, 732.

geometry of the isolated dimer and is therefore justifiably exaggerated in Figure 3. For H_2S, the contours again suggest hemisphericity, although there is a slight distortion along the symmetry-axis direction. Clearly, we must seek a more demonstrative way of delineating the directions of nonbonding pairs.

C. Evidence from the Electrostatic Potential in the Vicinity of Molecule B.—(i) *Contours of Equipotential.* Although the electron-density contour maps for *e.g.* H_2O show only slight distortion from sphericity, it is found that electrostatic potential contour maps are much more effective in locating nonbonding electron pairs. We are using the term electrostatic potential at a point here to mean the potential energy of a positive unit point charge ($+e$) at that point. It is assumed for this purpose that the proton ($+e$) does not perturb the charge distribution of B. The electrostatic potential contour map proves to be a more sensitive device for detecting the directions of nonbonding electron pairs than is the electron-density contour map. Thus, we show in Figure 9 the electrostatic potential contour map for the H_2O molecule, as derived from *ab initio* SCF calculations performed with minimal basis sets of Slater type orbitals by Scrocco and Tomasi.[55] Figure 9a shows the lines of equipotential appropriate to the H_2O symmetry plane σ_h. By contrast with the electron density diagram, the map in Figure 9a has the immediate advantage that it falls naturally into regions of positive and negative potential, thereby demonstrating clearly that one region near the molecule is electrophilic and the other is nucleophilic. We can understand qualitatively the electrostatic potential contours if we consider moving a proton on a circular path, starting at a point on the H_2O axis and beyond the oxygen nucleus. The potential at such a point is relatively large and negative, reflecting the displacement of electron density that leads to an electric dipole with its negative pole at the oxygen end of the molecule. As we move the proton on a semi-circular path the potential becomes less negative and eventually the effect of the positive poles at the hydrogen end of the molecule reduces the potential to zero. Then the effect of the positive pole becomes dominant and the potential begins to become increasingly positive.

In Figure 9b we show lines of equipotential appropriate to the perpendicular plane σ_v. It is striking that a unit positive point charge has a minimum potential energy (-73.7 kcal mol^{-1}) off the symmetry axis. There is no way of accounting for this by the dipolar model which, as seen above, provides a qualitative interpretation of the potential contours for the σ_h plane. Moreover, the line joining this point corresponding to the minimum to the oxygen nucleus makes an angle (φ) of $\sim 28°$ with the H_2O symmetry axis direction. By symmetry there is a second such minimum at $\varphi = -28°$ and these two minima are strongly suggestive of the directions of the nonbonding pairs on oxygen. Further evidence in support of such an association comes from considering the corresponding contour map for oxirane, which is shown in Figure 10 for the ring plane and the symmetry plane perpendicular to the plane of the ring.[55] Again, there are two symmetrically placed minima, the angle between which is now $2\varphi = 2 \times 48°$. This result is consistent

[55] E. Scrocco and J. Tomasi, *Top. Curr. Chem.*, 1973, **42**, 95.

with the familiar notion that the angle between the nonbonding electron pairs on oxygen in R_2O-type molecules increases as the ROR angle decreases (see Section 3C). The two examples of water and oxirane taken together provide evidence in favour of equipotential contour diagrams as a semi-quantitative means of locating nonbonding electron pairs. We shall discuss later why the angle for water is smaller than that ($\approx 54°$) predicted either from standard hybridization methods or from the valence-shell-electron-pair repulsion model.

(ii) *Evidence from Variation of the Electrostatic Potential with Angle at a Fixed Distance from B.* A chemically revealing way to recast the contour diagrams of Section 4C(i) is to plot the electrostatic potential $V(\varphi)$ at a fixed distance from B as a function of the angle φ. Such a plot is shown for H_2O at the distance $r = 1.74$ Å in Figure 11. [We have calculated $V(\varphi)$ with the aid of the distributed-point multipole model of H_2O given by Buckingham and Fowler[56]—see Section 4F]. We note that the curve is of the double-minimum type with a potential energy barrier to the $\varphi = 0$ position (point charge in the plane) of only 0.8 kJ mol^{-1} and with the minima at $\varphi = +30°$ and $\varphi = -30°$ when $r = 1.74$ Å which corresponds to the observed O···H distance in H_2O···HF.[10] This type of diagram clearly and simply reveals the directionality of the electrostatic potential. Moreover, the similarity of Figure 11 to Figure 2 is striking and indicates that, for H_2O···HF, the zeroth approximation in which HF is considered as merely $H^{\delta+}$ (*i.e.* a point positive charge) is not too unsatisfactory.

We next examine why the angle between the minima in Figure 11 is $2 \times \sim 30°$ instead of that expected on the basis of the nonbonding pair model of H_2O, *i.e.* $2 \times \sim 54°$. The reason for this is that the electrostatic potential at any point is determined only in part by the nonbonding pair in question but also in part by the resultant partial positive charge on the protons of H_2O and the negative charge of the other nonbonding pair. The partial positive charge will always act to decrease the potential of the point positive charge for a given angle φ and will become more effective as φ increases. On the other hand, the effect of the other nonbonding pair is that $V(\varphi)$ changes more slowly than expected as φ is reduced from $\varphi_{min.}$ to zero. Hence, $\varphi_{min.}$ will always be less than that expected on the basis of an isolated nonbonding pair. This effect is more serious in H_2O than in any other example that we consider because, first, the angle between the nonbonding pairs is smaller than in the other cases and, secondly, the O–H bond is short and strongly polar. We shall see below that for H_2S, for example, where $2\varphi_{min.}$ is large and the S–H bond is longer and less polar, $\varphi_{min.}$ is much closer to the expected value.

An analogous calculation of $V(\varphi)$ as a function of φ has been performed for H_2S but for several different values of r. The results are shown in the composite diagram in Figure 12. We note that while the height of the potential energy barrier between $\varphi = 0$ and $\varphi_{min.}$ is sensitive to r, the value of $\varphi_{min.}$ changes only slowly with r when varied from $r = 2$ Å, through $r = 2.33$ Å (the observed S···H distance in H_2S···HF[14]), to $r = 4.25$ Å, that is from $\varphi_{min.} = 80°$ to 65°. The value $\varphi_{min.} =$

[56] A. D. Buckingham and P. W. Fowler, *Can. J. Chem.*, 1985, **63**, 2014.

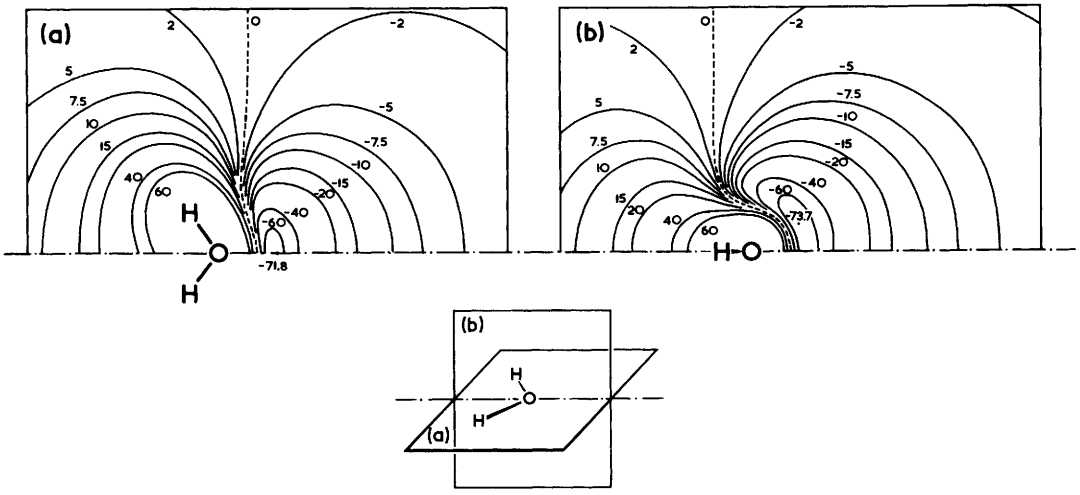

Figure 9 *Electrostatic potential-energy maps for* H_2O. (*a*) *shows lines of equipotential* (*in* kcal mol^{-1}) *appropriate to the* H_2O *symmetry plane* σ_h *while* (*b*) *is appropriate to the nonbonding-pair plane* σ_v
(Redrawn from ref. 55 with permission of Springer-Verlag)

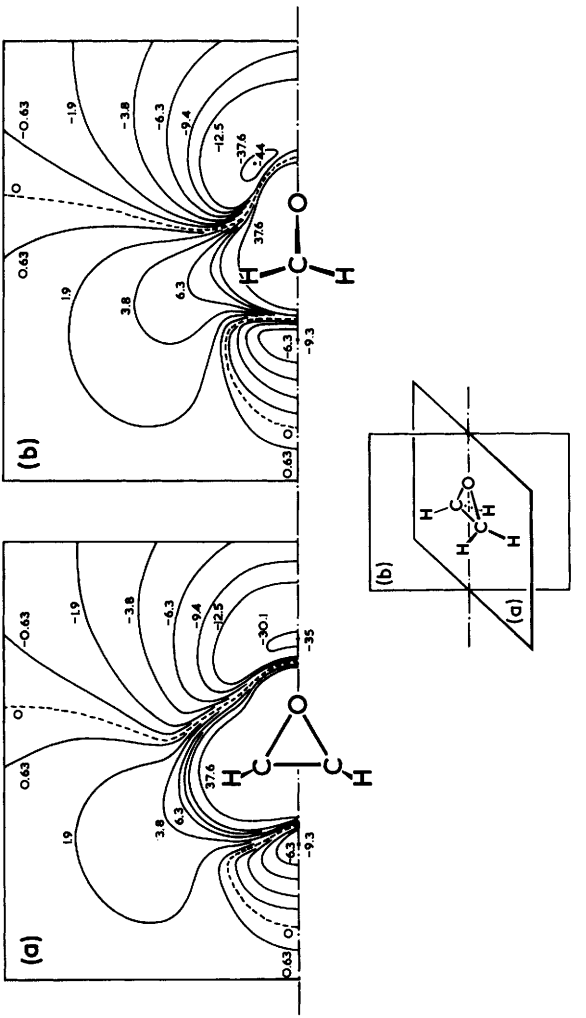

Figure 10 *Electrostatic potential-energy maps for oxirane.* (*a*) *shows lines of equipotential* (*in* kcal mol^{-1}) *appropriate to the oxirane symmetry plane* σ_h *while* (*b*) *is appropriate to the nonbonding-pair plane* σ_v.
(Redrawn from ref. 55 with permission of Springer-Verlag)

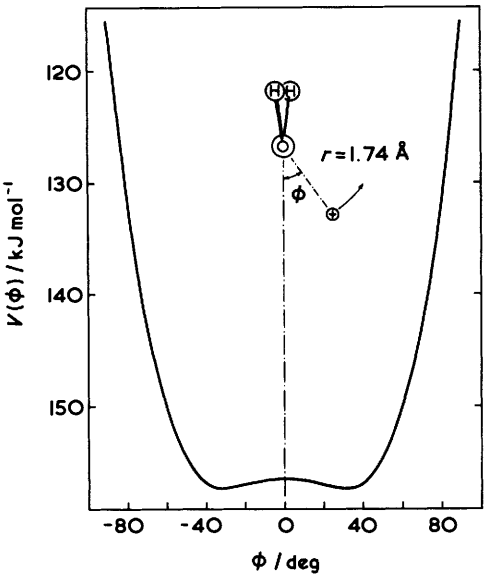

Figure 11 *Variation of the electrostatic potential energy $V(\varphi)$ with angle φ at a fixed radius r = 1.74 Å from the oxygen nucleus (the experimental O · · · H distance of H_2O · · · HF) in the vertical symmetry plane σ_v of H_2O. The sign ⊕ emphasizes that the potential $V(\varphi)$ is the energy of a nonperturbing point-positive charge at the defined point (r, φ)*

80° for r = 2.33 Å should be compared with the experimental angle $\varphi_{min.}$ = 89° for H_2S · · · HF and with the angle (90°) expected on the basis of the rules and the familiar hybridization model of H_2S. The relative insensitivity of $2\varphi_{min.}$ and the barrier height to r for H_2S (in contrast to the case of H_2O) arises because of the large angle between the nonbonding pairs on S and as a result the effect of each on a point positive charge is essentially isolated.

Another case in which the nonbonding pairs would be expected to be separated by a large angle ($\sim$120°) is formaldehyde. The corresponding diagram of $V(\varphi)$ for formaldehyde is given in Figure 13 for r = 1.794 Å [the experimental r(O · · · H) in H_2CO · · · HF[9]], where θ is defined as shown, with the point at a distance r from O confined to the plane of the formaldehyde molecule. Again, we find that $V(\theta)$ is of the double minimum type and that the angle $2\theta_{min.}$ is 80°. According to the usual nonbonding pair model of formaldehyde we would predict $2\theta_{min.}$ = 120°. For H_2CO · · · HF, the experimental angle C=O · · · F is 110°.

Finally, a similar approach for SO_2 leads to the potential energy curve $V(\theta)$ shown in Figure 14 for r = 1.892 Å [the experimental r(O · · · H) in SO_2 · · · HF].[16,17] Minima, which are not equivalent, fall at 150° and 230°. The simple nonbonding pair model of SO_2 has the axes of the pairs occurring at 120° and 240°, while the experimental result for SO_2 · · · HF corresponds to θ = 215°.

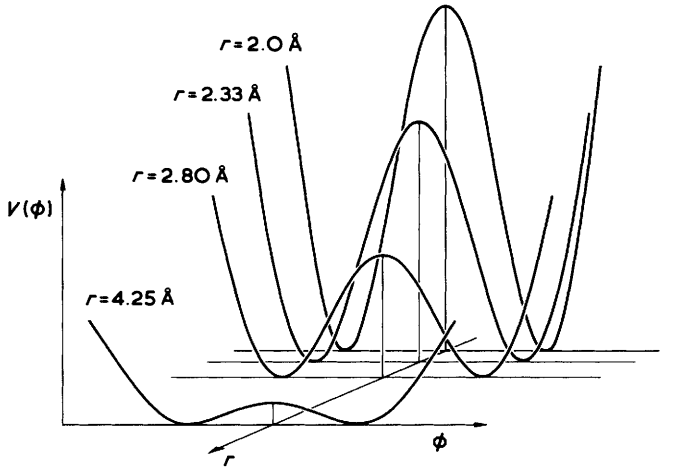

Figure 12 *A composite diagram of* $V(\varphi)$ *for* H_2S. *Each double-minimum curve shows the variation of* $V(\varphi)$ *with* φ *at a fixed radius r from the sulphur nucleus in the vertical symmetry plane* σ_v *of* H_2S. *r decreases from* 4.25 Å, *through* 2.8 Å, *and* 2.33 Å (*the experimental* S · · · H *distance in* $H_2S \cdots HF$) *to* 2.0 Å

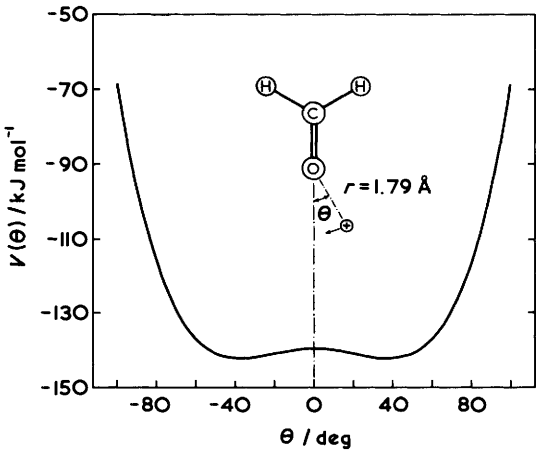

Figure 13 *Variation of the electrostatic potential energy* $V(\theta)$ *with angle* θ *at a fixed radius* $r = 1.79$ Å *from the oxygen nucleus in the horizontal symmetry plane* σ_h *of* H_2CO. *The experimental* O · · · H *distance in* $H_2CO \cdots HF$ *is* $r = 1.79$ Å

It is clear from the few representative examples of *n*-bonding acceptors discussed above (H_2O, H_2S, H_2CO, and SO_2) that the variation of the electrostatic potential at a fixed *r* with the angle φ or θ is a good semi-quantitative method of establishing the existence of and directionality of nonbonding electron pairs in acceptor molecules B.

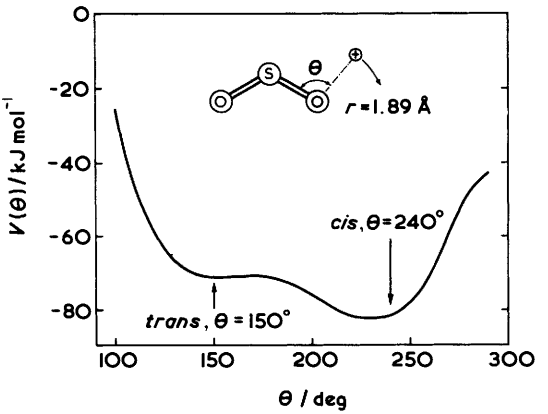

Figure 14 *Variation of the electrostatic potential energy $V(\theta)$ with angle θ at a fixed radius r = 1.89 Å from the oxygen nucleus in the horizontal symmetry plane σ_h of SO_2. The experimental O · · · H distance in SO_2 · · · HF is r = 1.89 Å*

Finally, a similar approach is possible for π-bonding acceptors such as acetylene and ethylene. Appropriate graphs of $V(\theta)$ *versus* θ show a single minimum at the expected angle $\theta = 90°$.

5 Electrostatic Models of the Hydrogen-bonded Dimer B · · · HX

A. Introduction.—Having in Section 4 presented evidence supporting the nonbonding and π-bonding electron pair model for the acceptor molecule B, we proceed in this Section to examine electrostatic models for the whole dimer B · · · HX. We shall for convenience refer to the case X = F throughout. In the simplest possible model of B · · · HF we can consider the angular geometry to be determined predominantly by the interaction of the $H^{\delta+}$ of HF with the electrostatic potential due to B, and therefore ignore completely the effect of F. We need discuss this model no further because the resulting angular geometries will be those defined by the potential energy minima discussed in Section 4C(ii) and, as indicated, these are (with the qualification about H_2O · · · HF already discussed) in good qualitative agreement with those predicted by the rules and observed experimentally.

The next stage in the development of the model is to consider HF to be an extended electric dipole with δ+ on H and δ− on F.

B. HF described as an Extended Electric Dipole in the Electrostatic Field due to B.—(i) *The model.* The next order of approximation is to consider not only the point charge δ+ on H in HF but also the point charge δ− on F, *i.e.* to consider HF as an extended electric dipole, and to calculate the electrostatic potential energy of this dipole in the electric field due to B. In practice, we do this by calculating the potential energy of two point charges $\delta+ = 0.54e$ and $\delta- = -0.54e$ (as suggested by the distributed point multipole model of HF given in ref. 56) and adding the two

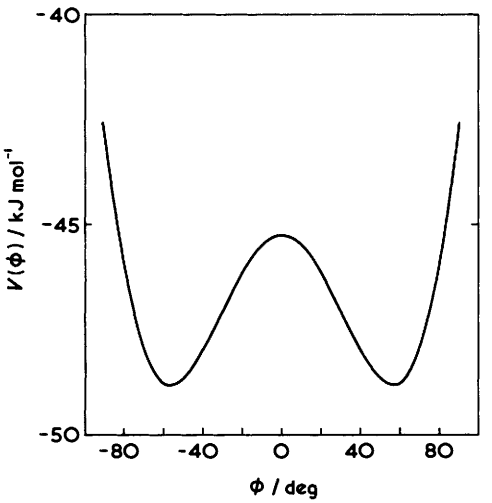

Figure 15 *Variation of the electrostatic potential energy $V(\varphi)$ with φ for* HF *in the vicinity of the oxygen atom of* H_2O *when* HF *is treated as an extended electric dipole* $\delta+ = 0.540e$ *on* H *and* $\delta- = 0.540e$ *on* F. *The* O • • • H *distance is* 1.74 Å *as in Figure* 11 *while the* HF *distance is the standard* r_0 *value*

contributions to give $V(\varphi)$ at a given angle φ and fixed distance r. The result for the case of $H_2O \cdots HF$ is shown in Figure 15. We note that the potential energy minimum for the system is now at $\varphi_{min.} = 55°$ which is within experimental error of the observed value $\varphi_{min.} = 46(8)°$. A similar approach for $H_2S \cdots HF$ leads to $\varphi_{min.} = 85°$ and for $H_2CO \cdots HF$ to $\theta_{min.} = 50°$. Both results are in good agreement with experiment (see Section 3C) and with the predictions of the crude model in Section 4C(ii).

(ii) *A corollary to the Rules.* Given the success of the above electrostatic model in which HF is treated as an extended electric dipole in the electric field due to B, we can propose a corollary to the rules for predicting angular geometries of B • • • HX discussed in Section 3B:

As long as the hydrogen bond in B • • • HF is sufficiently weak that (as implied above) the electric charge distributions of B and HF are essentially unperturbed, the HF axis acts as a probe for the direction of a nonbonding (or π-bonding) pair on B.

C. HF described by the Distributed Electrostatic Point-multipole Model.—We have discussed the electrostatic energy of a point charge in the potential due to B at a point (r, φ), for example, in the vicinity of B as a zeroth approximation to obtain the angular geometry of B • • • HF. In the next approximation we then considered HF as an extended electric dipole interacting with the electric field due to B. We refer now to more precise calculations of the electrostatic interaction[56] and we therefore use a more complete description of the electrostatic charge distribution of HF. In

principle the simplest quantitative electrostatic approach to the interaction between the monomers B and HX is to represent each by a molecular multipole expansion, assigning molecular dipole, quadrupole, and octupole moments to each of B and HX and then summing the electrostatic interaction energies given by the expansion. Unfortunately, for the distance of approach between B and HX in a typical hydrogen-bonded dimer, the series of terms does not converge. Following the work of Bernal and Fowler,[42] and Lennard-Jones and Pople,[43] there have been numerous attempts to model the electrostatic interaction between two monomers by distributing point charges or multipoles within the monomers. Brobjer and Murrell[57] have modelled simple molecules by locating point partial charges in a way which satisfies the molecular moments (dipole, quadrupole, octupole, and hexadecapole). The interaction between the point charges distributed over the two monomers is then readily calculated.[57] The angular variation of the energy at the observed hydrogen bond distance for a number of dimers leads to minima in accord with observed geometries.[57] These papers appear to be the first to give quantitative support to a relationship between electrostatic energy and geometry. Similarly, Kollman has made numerous calculations for hydrogen bonded dimers in terms of point charge distributions, including molecules as simple as water and as complex as deoxyribose or uracil.[58] Pullman and Perahia[59] on the other hand have used sets of multipoles (point monopoles, dipoles, and quadrupoles) distributed over the molecular geometry to investigate processes such as the hydration of uracil. Bentley[60] has shown how molecular charge densities may be represented for small molecules by point multipoles centred on the constituent atoms. Such atom-centred point-multipole descriptions reproduce the molecular moments and allow electrostatic potentials to be calculated at large and intermediate distances. Hirshfeld has also tabulated distributed multipole moments at atom centres for a number of small molecules.[61] Stone[62] has introduced a distributed point multipole description of electronic charge distributions in which point multipoles are placed on atoms and at the centres of bonds. Buckingham and Fowler[56] have evaluated, and conveniently tabulated, such distributed point multipoles for a number of simple molecules, for the most part placing multipoles on the atoms of the molecule and in some cases at the centres of bonds. Buckingham and Fowler then find the minimum electrostatic energy of interaction of B and HX by use of a model in which these multipoles are embedded in hard van der Waals spheres. The spheres represent the short-range repulsion and determine the hydrogen-bond length at which the electrostatic interaction energy between the sets of distributed multipoles representing each monomer is to be determined. In almost all cases where an experimental structure is known this electrostatic model proves quantitatively

[57] J. T. Brobjer and J. N. Murrell, *J. Chem. Soc., Faraday Trans. 2*, 1982, **78**, 1853; 1983, **79**, 1455; *Chem. Phys. Lett.*, 1981, **77**, 601; J. T. Brobjer, *Faraday Discuss. Chem. Soc.*, 1982, **73**, 123; 128.
[58] U. C. Singh and P. A. Kollman, *J. Computat. Chem.*, 1984, **5**, 129.
[59] A. Pullman and D. Perahia, *Theochem. Acta*, 1978, **48**, 29.
[60] J. Bentley in 'Chemical Applications of Atomic and Molecular Electrostatic Potentials', ed. P. Politzer and D. G. Truhlar, Plenum Press, New York, 1981, p. 63.
[61] F. L. Hirshfeld, *Theor. Chim. Acta*, 1977, **44**, 129.
[62] A. J. Stone, *Chem. Phys. Lett.*, 1981, **83**, 233.

correct. We note that for $H_2O \cdots HF$ the Buckingham–Fowler model leads to $\varphi_{min.} = 60°$, which is close to the experimental value and also to the value obtained with HF considered merely as an extended electric dipole.

D. Quantum Mechanical Justification of the Electrostatic Model for Angular Geometries of B • • • HX.—Recently, strong support for the electrostatic model has been obtained by a comparison of its predictions with the results of *ab initio* calculations for a number of carefully chosen dimers.[52] The quantum mechanically calculated interaction energy is partitioned into electrostatic, exchange, polarization, and charge-transfer contributions. The results of the calculations show that the electrostatic contribution is generally the dominant factor in determining both the strength and the angular geometry of the complex and that the angular dependence of the electrostatic contribution parallels that obtained from the point multipole model. As an example, Figure 16 shows the variation with φ of the various contributions to the energy for $H_2O \cdots HF$, as determined from the *ab initio* calculation. It is seen that the electrostatic term dominates the angular dependence of the interaction energy in this sensitive case and that the model electrostatic energy closely parallels the electrostatic term in the quantum mechanical calculation. The polarization energy is very small and almost entirely independent of φ. A similar behaviour was found[52] in several other dimers. This justifies the implicit assumption throughout this article that polarization of one molecule by the other has a negligible effect on angular geometries of B • • • HX.

6 Further Applications of the Electrostatic Model

A. Introduction.—The electrostatic model has been shown to account well for angular geometries of hydrogen-bonded dimers and clearly has predictive value. We shall indicate in this Section that the electrostatic model, or an extension of it, can account for a number of other properties of hydrogen-bonded dimers and thus can now be seen as providing a useful basis for thinking generally about hydrogen bonding. We illustrate this by considering the following properties: hydrogen-bond stretching and bending force constants, HF bond lengthening in dimers B • • • HF, deviations from linearity of B • • • H–X hydrogen bonds, and the extent of proton transfer from HX to B. Finally, we examine briefly the applicability of the simple rules to hydrogen-bond angular geometries in the solid state.

B. Stretching Force Constant k_σ of Hydrogen Bonds.—Spackman[63] has combined the use of distributed moments for the calculation of electrostatic interactions with the use of atom–atom potentials for the representation of repulsion and dispersion energies to obtain a model for the quantitative estimation of dimer properties. The atom–atom potentials are taken to be of the exp-6 form but with the omission of the exp-6 terms between the proton and its acceptor. The model has been applied to the calculation of hydrogen-bond stretching force constants, k_σ, of dimers formed by linear molecules, using Hirshfeld's partitioning scheme[61] for the computation of the

[63] M. A. Spackman, *J. Chem. Phys.*, 1986, **85**, 6587.

Table 2 *Observed and calculated values of* k_σ/N m^{-1} *for dimers* B · · · HX

	Calc.[a]	*Exp.*[b]		*Calc.*	*Exp.*		*Calc.*	*Exp.*
N_2 · · · HF	5.7	5.5	N_2 · · · HCl	3.6	2.5	N_2 · · · HCN	3.1	2.3
OC · · · HF	10.7	8.5	OC · · · HCl	6.0	3.9	OC · · · HCN	5.0	3.3
HCN · · · HF	24.6	18.2	HCN · · · HCl	14.9	9.1	HCN · · · HCN	14.1	8.1
HCCCN · · · HF	18.0	16.3	HCCCN · · · HCl	11.1	—	HCCCN · · · HCN	—	—

[a] Calculated values taken from reference 63. [b] Experimental values are taken from reference 37

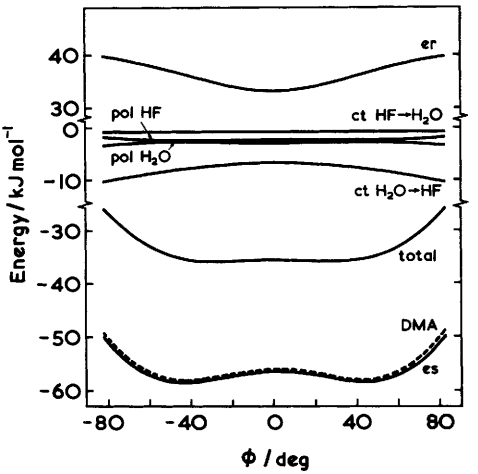

Figure 16 *Calculated intermolecular energies for* H_2O · · · HF *as a function of* φ. *The total* ab initio *perturbation value is indicated by 'total' and the following labels indicate the partitioning of this energy: es, accurate electrostatic energy; er, exchange repulsion energy; pol, polarization energy for molecule indicated; ct, charge transfer energy in the direction indicated. DMA refers to the electrostatic energy evaluated according to the distributed point-multipole model* (Redrawn, with permission, from ref. 52)

distributed moments for the linear monomer molecules. Table 2 compares k_σ values so calculated[63] with those determined experimentally[37] for selected dimers B · · · HX. The agreement between the two sets provides support for this extension of the simple electrostatic model.

C. Bending Force Constants of Hydrogen-bonded Dimers.—Bending force constants of hydrogen-bonded dimers have proved more difficult to obtain experimentally than hydrogen bond stretching force constants. The most complete determination of the quadratic bending force constants for a hydrogen-bonded dimer so far obtained is that for MeCN · · · HF.[64] Less well established bending force constants are available for HCN · · · HF[2] and H_2O · · · HF,[65] and a limited amount of information has also been reported for a range of dimers B · · · HX (X = F, Cl, CN)

[64] A. C. Legon, D. J. Millen, and S. C. Rogers, *J. Mol. Struct.*, 1980, **67**, 29.
[65] Z. Kisiel, A. C. Legon, and D. J. Millen, *J. Mol. Struct.*, 1984, **112**, 1.

from a study of vibrational amplitudes obtained from the analysis of hyperfine structure in dimer spectra.[66] From the measurements available it appears that for bending B · · · HX at B the restoring force constant is generally small while that for bending at the hydrogen atom is appreciably larger. Thus the values for MeCN · · · HF are[64] respectively 2.4×10^{-20} and 8.0×10^{-20} J rad^{-2}, and for H_2O the corresponding values are 2.52×10^{-20} and 9.85×10^{-20} J rad^{-2} respectively.[65] Thomas[67] has pointed out that according to a dipole–dipole model the two force constants would be expected to be equal.

Nevertheless while the dipole–dipole model fails, the origin of the significant difference in the two bending force constants can readily be understood qualitatively in terms of an electrostatic model by reference to Figure 17 which considers as an example H_2O · · · HF. Figure 17(a) shows the HF molecule at its equilibrium position in the electrostatic potential contour diagram.[55] Figure 17(b) illustrates the relative positions of H_2O and HF for bending at O, which to a first approximation describes the bending mode ν_β. It is seen qualitatively that the potentials at H and F are little changed as a result of bending, the HF molecule moving relative to H_2O on a path which approximately parallels the contours. Only small deviations from hemisphericity in the contours occur over the vibrational amplitude and the restoring force constant is consequently small. Indeed for Ar · · · HF this mode disappears. By contrast the motion in the bending mode ν_B [see Figure 17(c)] causes the hydrogen atom to move on an arc cutting across the potential contours, leading to a significantly larger restoring force constant for this motion. Thus while both of the modes ν_β and ν_B for H_2O · · · HF involve essentially hydrogen motion, the former falls at 157 cm^{-1} and the latter at 696 cm^{-1}.[65]

D. HF Bond Lengthening on Formation of B · · · HF.—Recently it has been shown[68] how nuclear hyperfine structure in microwave spectra of dimers B · · · HF can be used to determine the lengthening δr of the HF bond on formation of dimers B · · · HF, where B = N_2, CO, H_2S, HCN, MeCN, or H_2O. A simple electrostatic model proves to be capable of predicting such lengthenings and the results are found to be in good agreement with experimental values where these are available.

Table 3 *Comparison of experimental and calculated* HF *bond lengthenings* δr *in a series of dimers* B · · · HF

B	δr_{obs}/Å	δr_{calc}/Å
N_2	0.002	0.0041
CO	0.007	0.0076
H_2S	0.010	0.0106
HCN	0.016	0.0150
MeCN	0.017	0.0153
H_2O	0.017	0.0203

[66] P. Cope, D. J. Millen, and A. C. Legon, *J. Chem. Soc., Faraday Trans. 2*, 1986, **82**, 1189.
[67] R. K. Thomas, *Proc. R. Soc. London, Ser. A*, 1975, **344**, 579.
[68] A. C. Legon and D. J. Millen, *Proc. R. Soc. London, Ser. A*, 1986, **404**, 89.

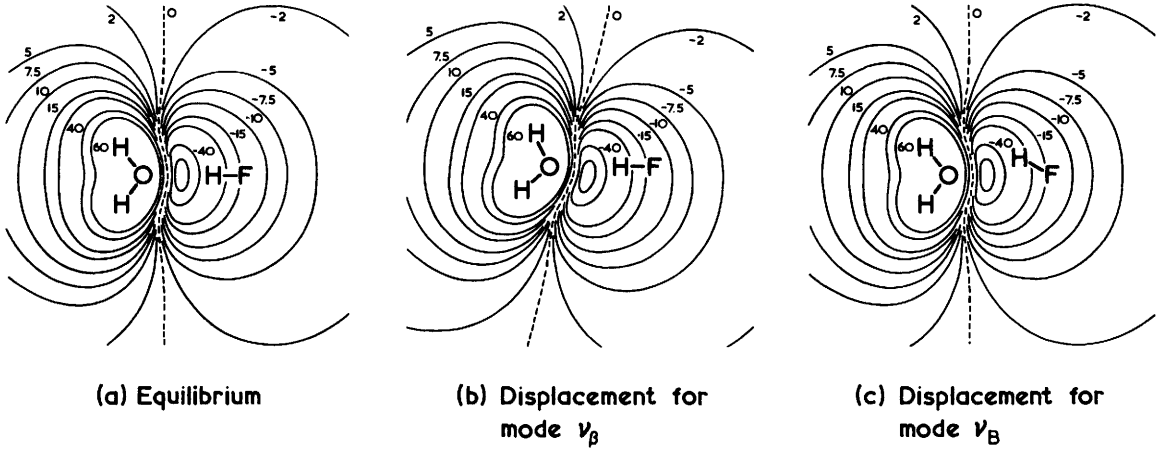

Figure 17 *Electrostatic potential energy diagrams used to illustrate the relative ease for angular distortions from (a) equilibrium and approximating to (b)* ν_β *and (c)* ν_B*, where* ν_B *and* ν_β *are the in-plane high- and low-frequency hydrogen-bonding bending modes, respectively, in* $H_2O\cdots HF$

The simple model of the dimer B···HF takes as its starting point the representation of the HF molecule used in Section 5B, namely an extended dipole having point charges $\delta+ = 0.54e$ and $\delta- = -0.54e$ located at the H and F nuclear positions, respectively. The acceptor B is accurately represented electrostatically by a point multipole model.[56] The resultant attractive force f_H on the hydrogen end of the HF dipole is then readily evaluated, as is the corresponding repulsive force f_F on the fluorine end of the dipole. The bond lengthening in the harmonic oscillator approximation is taken to be given by

$$k_S \delta r = f_H$$

where k_S is the quadratic force constant for HF in the dimer. Implicit in this equation is the assumption that the hydrogen atom can move towards B as a result of the force acting on it. As discussed by a number of authors, the hydrogen atom appears to experience no repulsive interaction with B at the distances normally found for hydrogen-bonded dimers. The most recent of discussions, that by Spackman,[63] has already been referred to in Section 6B.

The values of δr calculated from the model for a series of dimers B···HF are compared with the experimental values in Table 3. Calculated values are plotted as solid circles in Figure 18 and experimental values are shown as open circles. The hydrogen-bond stretching force constant k_σ has been used as a convenient measure of hydrogen bond strength. It is seen that the model leads to remarkably good agreement with experiment given the simplicity of the approach for calculating δr and the assumptions made in obtaining δr indirectly from experimental hyperfine coupling constants. The model predicts a bond lengthening $\delta r = 0.040$ Å for H_3N···HF. No experimental value is available for comparison but the result is in reasonable agreement with the value of 0.028 Å obtained by Scheiner *et al.*[69] from *ab initio* calculations.

E. Deviations from Linearity of Hydrogen Bonds in B···HX.—Deviations from linearity of hydrogen bonds B···H–X are difficult to establish by microwave spectroscopy. In the case of HCN···HF there is good evidence that the dimer has a linear equilibrium geometry[2] and this is consistent with all theoretical calculations. On the other hand, for less symmetrical acceptors B, theoretical calculations often show small deviations from linearity. Thus for H_2O···HF Buckingham and Fowler[56] find the equilibrium geometry shown in Figure 19(a). The deviation from linearity of OHF can be understood qualitatively by reference to the potential contour diagram in Figure 9. Movement of the fluorine atom off the O···HF axis in the direction shown in the diagram is seen to move it into a region of lower negative potential, and thus deviation from linearity in this direction is electrostatically favoured. We have already seen that the negative potential falls of in this direction because of the influence on the potential of $\delta+$ located by the model

[69] Z. Latajka and S. Scheiner, *J. Chem. Phys.*, 1984, **81**, 1166.

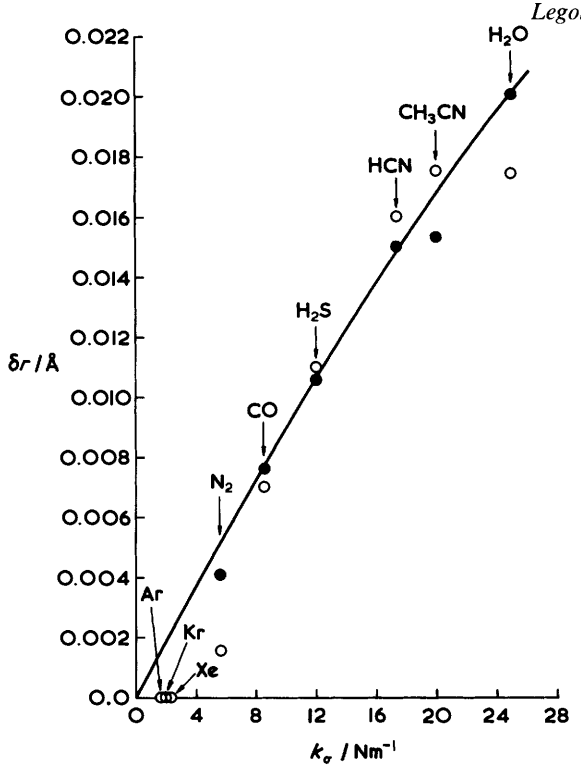

Figure 18 *Experimental values* (○) *and calculated values* (●) *of the* HF *bond lengthening* δr *on forming* B···HF *plotted against* k_σ, *the hydrogen bond stretching force constant*

on the hydrogen atoms, so in more chemical language we can say that the deviation from linearity arises from the attraction exerted on the fluorine atom by hydrogen atoms of the water molecule.

Buckingham and Fowler[56] also find deviations of the hydrogen bond from linearity of a similar magnitude in other dimers. For example, the deviations are 9° and 7° in $H_2CO \cdots HF$ and $HF \cdots HF$, respectively. Direct experimental evidence for such small distortions is difficult to obtain because of the well-known problems of locating an H atom near the centre of mass by rotational spectroscopy. On the other hand, it is worth noting that along the series $H_2S \cdots HX$ where the angular geometry is of the general type shown in Figure 19(b) the angle φ has the values 84.5°, 89°, 93.8°, and 96.5° when X = CN, F, Cl, and Br,[70] respectively. Evidently, this variation in angular geometry has an electrostatic origin since the order in φ can be rationalized if we assume that the charge $\delta+$ on H in H_2S is attracted to the group X with increasing strength along the series. Indeed, Buckingham and Fowler find quantitative agreement with experiment for X = CN, F, and Cl using their electrostatic model.

[70] A. I. Jaman and A. C. Legon, *J. Mol. Struct.*, 1986, **145**, 261.

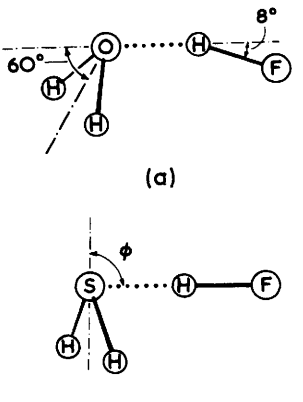

Figure 19 (*a*) *Deviation of the hydrogen bond from linearity in* $H_2O \cdots HF$ *as calculated by the Buckingham–Fowler method.* (*b*) *Deviations from* $\varphi = 90°$ *in some experimentally determined angular geometries for* $H_2S \cdots HX$. *The values of* φ *are* 84.5°, 89°, 93.8°, *and* 96.5° *for* X = CN, F, Cl, *and* Br, *respectively*

F. Is there a Substantial Contribution $\overset{+}{B}H\ \overset{-}{X}$ to the Valence-bond Description of BH • • • X?—The discussion so far in this article has assumed implicitly that gas-phase hydrogen-bonded dimers can be described as $B \cdots HX$, with only a negligible contribution from the valence-bond structure $\overset{+}{B}H\ \overset{-}{X}$ (*i.e.* negligible proton transfer). Can this assumption be justified?

Recently, we have examined[71,72] how the Cl-nuclear quadrupole coupling constant χ(Cl) (as determined by rotational spectroscopy) varies along the series of dimers $B \cdots H^{35}Cl$ where, in order of increasing binding strength, B = OC, C_2H_4, C_2H_2, H_3P, H_2S, HCN, MeCN, H_2O, or H_3N. χ(Cl) is an important property of the dimer because it provides a measure of the electric field gradient at the Cl nucleus and therefore contains information about the electrical changes that occur in HCl on formation of $B \cdots HCl$. We find we can account entirely for the observed value χ(Cl) in all cases (including $H_3N \cdots HCl$) by a simple electrostatic model that allows only for the additional electric field gradient at Cl in $B \cdots HCl$ arising from B, with no proton transfer between the subunits. Thus, we write the equilibrium value χ_e(Cl) of the coupling in the equilibrium form of the dimer

$$\chi_e(\mathrm{Cl}) = -(eQ/h)\{\mathbf{F}_{zz}F_z + \mathbf{G}_{zz}F_{zz}\} + (\partial\chi_0/\partial r)\delta r \qquad (1)$$

where $(\partial\chi_0/\partial r)\delta r$ allows for the effect of a small lengthening δr of the HCl molecule on formation of the dimer and where $\mathbf{F}_{zz}F_z$ is the electric field gradient at Cl arising from the action on HCl of the electric field F_z due to B (*i.e.* from the polarization of HCl by B) while $\mathbf{G}_{zz}F_{zz}$ is correspondingly that resulting from the electric field

[71] P. Cope, A. C. Legon, and D. J. Millen. *J. Chem. Soc., Faraday Trans. 2*, 1987, **83**, 2163.
[72] A. C. Legon and D. J. Millen, *Proc. R. Soc. London, Ser. A*, to be published.

gradient F_{zz} at Cl due to B but enhanced by Sternheimer antishielding. After calculating F_z and F_{zz} from the distributed point multipole model of B, we find that when the best available value of the Sternheimer factor for HCl is used in equation 1, after suitable zero-point averaging, the same value of $\mathbf{F}_{zz}$ is obtained for each member of the series B $\cdots$ HCl even though the strength of the intermolecular binding (as measured by the intermolecular stretching force constant k_σ) increases by a factor of five from B = CO to NH_3. This provides convincing evidence that our model is satisfactory, *i.e.* that the change $\Delta\chi_0$ in the Cl-nuclear quadrupole coupling constant for each member of the series is completely described by the simple model, with no need to invoke significant contributions from the ionic structure $\overset{+}{B}H\ \overset{-}{Cl}$ even for $H_3N \cdots HCl$.

G. Angular Geometries for Hydrogen-bonding in the Solid State.—It is to be expected that generalizations from gas-phase studies of hydrogen bonding will have important implications for understanding hydrogen-bonding in condensed phases. Thus the general finding that bending of a hydrogen bond at the heavy atom is relatively easy to bring about while bending at the hydrogen atom is more strongly resisted (see Section 6C) is directly relevant to understanding distortions from nonbonding pair geometries in the liquid and solid states. Distortions from the nonbonding pair axis can readily occur at the demand of the hydrogen bond environment, while distortions leading to bent hydrogen bonds are energetically much less probable. Applications of these ideas can be made to hydrogen bonding to both $>$O and $>$C=O groups in the solid state. Statistical analyses of large numbers of *X*-ray diffraction[73] and neutron diffraction[74] investigations for hydrogen bonds of the type $>O \cdots H–O$ show that while there is some preference for hydrogen bonding in the plane containing the axes of the nonbonding pair of the acceptor oxygen atom, there is no favoured angle for hydrogen bond formation in that plane. It has been indicated[65,75] that these are just the results to be expected if the bending potential energy functions are of the same form as those for $H_2O \cdots HF$, where the out-of-plane bending motion is governed[7] by a double minimum potential energy function with a barrier of only $\sim$1.5 kJ mol^{-1} (see Figure 2) while the in-plane bending is governed by a much narrower single minimum potential function.[65] Thus the interpretation of the diffraction results is that for $>O \cdots H–O$ hydrogen bond lattice effects are large compared with distortion in the plane of the nonbonding pair axes, but not so large as to eliminate the configurational preference for the plane. By contrast, statistical analyses[76] of large numbers of *X*-ray diffraction results for $>C=O \cdots H–N$ hydrogen bonds show a significant tendency for hydrogen-bonding to occur in the directions of the conventionally viewed oxygen sp^2 nonbonded pairs. This result has led to the expectation[77] that the barrier height in the double-minimum bending potential

[73] J. Kroon, J. A. Kanters, J. G. C. M. van Duijneveldt, F. B. Duijneveldt, and J. A. Vliegenthart, *J. Mol. Struct.*, 1975, **24**, 109.
[74] C. Ceccarelli, G. A. Jeffrey, and R. Taylor, *J. Mol. Struct.*, 1981, **24**, 109.
[75] D. J. Millen, *Croat. Chem. Acta*, 1982, **55**, 133.
[76] R. Taylor, O. Kennard, and W. Versichel, *J. Am. Chem. Soc.*, 1983, **105**, 5761.
[77] D. J. Millen, *Int. J. Quantum Chem.*, 1986, **29**, 191.

energy function for hydrogen bonds involving the C=O group is significantly greater than is the case for hydrogen bonds to the >O group. Subsequent experiment[78] and *ab initio* calculation[52] have confirmed that the barrier height for the CH_2O,HF dimer is indeed significantly greater than that for the H_2O,HF dimer. Finally, both the *X*-ray[73] and the neutron diffraction[74] studies for hydrogen bonds to the >O group show that, when proper account is taken of weighting, hydrogen bonds bent at the hydrogen atom by more than 15° are exceptional in these systems, while large angular deviations at the oxygen atom from the directions of the nonbonding axes are common. These results are entirely consistent with expectations outlined above.

7 Conclusion

A wealth of experimental evidence about isolated hydrogen-bonded dimers B • • • HX has been gathered over the last decade,[3,51,79] mainly through rotational spectroscopy, and has allowed several generalizations about such dimers. In particular, a set of rules based on the *n*-bonding and π-bonding electron pairs in the acceptor molecule B have been enunciated and the angular geometries successfully predicted. These rules are essentially electrostatic in origin, for they imply that the electrophilic hydrogen atom of HX seeks regions of high electron density in B (*e.g.* the directions of *n*-bonding and π-bonding pairs). The rules have been followed by the development of a quantitative electrostatic model[56] which has also been very successful in accounting for angular geometries and which rests on the distributed point-multipole model as an accurate and reliable method for calculating electrostatic interactions.[62] Further justification of the quantitative electrostatic model has been provided by intermolecular perturbation theory.[52] We have also shown in this article how a number of properties other than the angular geometry can be understood in terms of a simple electrostatic approach to the nature of the hydrogen bond.

Acknowledgement. We are pleased to acknowledge research grants from S.E.R.C. in support of our work on hydrogen bonding.

[78] F. J. Lovas, R. D. Suenram, S. Ross, and M. Klobukowski, *J. Mol. Spectrosc.*, 1987, **123**, 167.
[79] A. C. Legon and D. J. Millen, *Acc. Chem. Res.*, 1987, **20**, 39.